



# Synthesis and conformational studies of pseudopeptides containing an unsymmetrical triazine scaffold

ERIKA BOURGUET,<sup>a</sup> ISABELLE CORREIA,<sup>b</sup> BERTRAND DORGERET,<sup>a</sup> GERARD CHASSAING,<sup>b</sup> SAMES SICSIĆ<sup>a</sup> and SANDRINE ONGERI<sup>a\*</sup>

<sup>a</sup> Université Paris-Sud XI, BioCIS UMR-CNRS 8076, Molécules Fluorées et Chimie Médicinale, IFR 141, Faculté de Pharmacie, 5 rue Jean-Baptiste Clément, 92296, Châtenay-Malabry Cedex, France

<sup>b</sup> UMR-CNRS 7613, Synthèse, Structure et Fonction de Molécules Bioactives, Université Pierre et Marie Curie, boîte 45, 4 place Jussieu, 75252 Paris Cedex 05, France

Received 9 July 2007; Revised 23 August 2007; Accepted 25 August 2007

**Abstract:** Solid-phase synthesis and conformational studies of two pseudopeptides constituted by a triazine scaffold bound to two peptidic arms are described. In this paper, a new scaffold based on unsymmetrical triamino 1,3,5-triazine bearing two alkyl chains has been designed, assisted by molecular modelling, as a mimic of the backbone of the  $i + 1$  and  $i + 2$  residues of a  $\beta$ -turn. The results confirm the ability of the triazine scaffold to induce extended conformations of the peptidic strands and point out that this scaffold is a good candidate as a template to induce anti-parallel  $\beta$ -sheet structure. Copyright © 2007 European Peptide Society and John Wiley & Sons, Ltd.

Supplementary electronic material for this paper is available in Wiley InterScience at <http://www.interscience.wiley.com/jpages/1075-2617/suppmat/>

**Keywords:** solid-phase; molecular modelling; conformation analysis; peptidomimetic; triazine;  $\beta$ -turn

## INTRODUCTION

Inappropriate mutations of normal cellular proteins are known to generate fragmentary peptides or abnormal disease-causing isoforms. More particularly, a series of pathological processes is linked with the formation of a  $\beta$ -sheet structure in various internal organs and consecutive protein aggregation in the form of  $\beta$ -amyloid deposition, causing functional diseases called amyloidosis. In amyloids,  $\beta$ -sheets are made up of  $\beta$ -strands that are oriented perpendicular to the fibril axis in an arrangement called a cross  $\beta$ -structure [1–5]. Amyloids are said to be the primary cause for Alzheimer's disease [6,7]. Furthermore, the conversion of  $\alpha$ -helices to larger  $\beta$ -sheet aggregates is found in Creutzfeldt-Jakob disease, BSE, and other prion diseases [8–10]. In Parkinson's disease,  $\alpha$ -sinuclein which is normally in an unfolded state, forms oligomers of  $\beta$ -sheets which lead to amyloid fibrils [11]. Islet amyloid deposits are present in over 85% of type 2 diabetic patients, and it has been suggested that they may be pathogenic [12–14]. Despite their abundance and dramatic progression there is virtually no therapy for protein misfolding diseases. Therefore a better understanding of the mechanism of aggregation and

the development of possible  $\beta$ -sheet ligands, which can slow down or prevent the pathological process, is of great interest from both a mechanistic and a therapeutic point of view. Because the amyloid contains a large amount of  $\beta$ -sheet structure, it is a challenge to synthesize  $\beta$ -sheet assemblages to understand the pathogenesis and the therapeutics of these diseases.

While  $\beta$ -sheet structure is commonly observed in proteins, our understanding of this structural motif is poor compared to what is known about  $\alpha$ -helical secondary structure. This is due in part to the difficulties inherent in creating a well-defined peptide model system for the study of  $\beta$ -sheet formation in aqueous solution. The use of small hydrophobic oligopeptides or amphiphilic oligopeptides as models for  $\beta$ -sheet structure has generally resulted in the formation of heterogeneous  $\beta$ -sheets which self-associate and precipitate [15,16]. In most cases the handling and purification of these peptides have proven to be very difficult [17].

In 1988, Kemp and Bowen [18–20] reported the synthesis of the first well-defined model for the formation of anti-parallel  $\beta$ -sheet with conjugates of short polypeptides and 2,8-diaminoepindolidione. Since then,  $\beta$ -strand peptidomimetics have attracted attention. For example, Martin and co-workers developed 1,2,3-trisubstituted cyclopropanes as peptide isosteres that mimic  $\beta$ -strand conformation [21]. Hirschmann designed 3,5-linked pyrroline-4-ones [22–24] and Schrader reported that aminopyrazole oligomers were

\*Correspondence to: Sandrine Ongeri, Université Paris-Sud XI, BioCIS UMR-CNRS 8076, Molécules Fluorées et Chimie Médicinale, IFR 141, Faculté de Pharmacie, 5 rue Jean-Baptiste Clément, 92296, Châtenay-Malabry Cedex, France; e-mail: Sandrine.Ongeri@u-psud.fr

able to stabilize inter-molecular  $\beta$ -sheets [25–28]. However only a few  $\beta$ -sheet peptidomimetics have been described. About ten years ago, Kelly used a dibenzofuran derivative as a  $\beta$ -turn model and examined the formation of a  $\beta$ -sheet structure in aqueous solution [29,30]. More recently this author used biphenyl derivatives to mimic  $\beta$ -turns [31,32]. Since 1992, Nowick *et al.* has been reporting on the development of an oligourea ‘molecular scaffold’ designed to hold multiple peptide or peptidomimetic strands based on 5-amino-2-methoxybenzamides [33–38]. More recently, norbornane and norbornene motifs have also been studied as scaffolds for  $\beta$ -sheet conformation of peptides [39–41].

We present in this report a new triamino 1,3,5-triazine scaffold as a candidate for a template to induce anti-parallel  $\beta$ -sheet structure. For this, we describe the synthesis using a solid-phase technique, and the structural analysis using NMR spectroscopy of two pseudopeptides containing unsymmetrical triamino 1,3,5-triazine.

## RESULTS AND DISCUSSION

The challenge for creating a synthetic anti-parallel  $\beta$ -sheet is to find a scaffold which is able to orientate correctly, two peptidic arms allowing them to interact by creating an array of alternate 10- and 14-membered hydrogen bond rings. Another challenge is to create a  $\beta$ -sheet soluble in a solvent compatible with biological tests, water or possibly methanol or ethanol. However peptidic  $\beta$ -sheets are known to be very hydrophobic because it is well established that hydrophobic amino acids favour  $\beta$ -sheet formation [42].

We decided to focus our study on a scaffold based on triamino 1,3,5-triazine (melamine) bearing two peptidic arms connected to the scaffold through alkyl chains (Figure 1). The triamino 1,3,5-triazine scaffold was chosen because it might replace a  $\beta$ -turn by mimicking the backbone of the  $i+1$  and  $i+2$  residues of a  $\beta$ -turn and therefore, by reversing the polypeptide chain direction. This scaffold was chosen also because of the synthetically easy access to unsymmetrical triamino 1,3,5-triazines from cyanuric chloride. Triamino 1,3,5-triazine derivatives have been widely reported previously as triazine-based macrocyclic scaffold [43–49], building blocks for dendrimers [50,51], or molecules with biological activities [52–56]. The stepwise substitution of the triazine ring is well documented and so, by controlling the temperature, the sequential addition of amines to cyanuric chloride generates trisubstituted melamines with typically high yields [43–56].

We had then to set up the nature, the length ( $m$ ), the orientation of the peptidic arms, and the length ( $n$ ) of the alkyl chains (Figure 1). We estimated that we

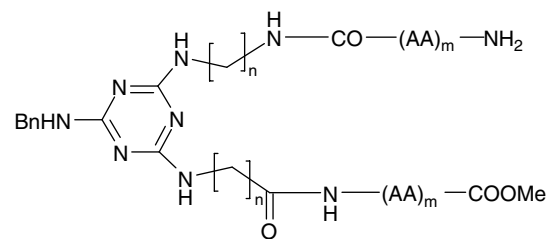


**Figure 1** Structure of pseudopeptides containing unsymmetrical triazine scaffolds.

needed at least four amino acids on each arm bound to our triazine scaffold to test its capacity to form a  $\beta$ -sheet structure. We chose hydrophobic amino acids as it is established that they favor  $\beta$ -sheet formation [42]. To set up the length ( $n$ ) of the alkyl chains and the direction of the peptidic arms we used molecular modelling tools (Molecular modelling of the two molecules was performed using the Sybyl 6.9 package of Tripos, and the MMFF94s force field. The molecules were constructed from a two-strand anti-parallel  $\beta$ -sheet structure of the PDB, containing four amino acids for each strand. These  $\beta$ -strands were conveniently bound to the triazine spacer, and each amino acid residue of the resulted structure was mutated to the corresponding amino acid of the desired molecules. The obtained molecules were minimized using a cut off 8, a dielectric constant 1, and a convergence gradient  $0.1 \text{ kcal mol}^{-1} \text{ \AA}^{-1}$ . Molecular dynamics studies were performed at 300 °K for each molecule using the default setup of Sybyl. These temperatures were gradually attained by seven steps of 40 °K and a last step of 20 °K, and the molecular dynamics (MDs) were continued for 50 000 fs, unless otherwise stated). Molecules  $A_{1-3}$  which contain the series  $G_1V_2A_3V_4$  and  $V_5K_6V_7F_8$  and molecules  $B_{1-3}$  which contain the opposite series  $V_1K_2V_3F_4$  and  $G_5V_6A_7V_8$  were studied (Figure 2). Molecules  $A_{1-3}$  and  $B_{1-3}$  were submitted to molecular dynamics (MDs) at 300 °K to test their ability to form a  $\beta$ -sheet structure, and their conformational stability.

In series A, only molecule  $A_2$  ( $n = 3$ ) (**1**) seemed to adopt a  $\beta$ -sheet structure with three hydrogen bonds ( $V_4 \text{ CO}-V_5 \text{ NH}$ ,  $V_4 \text{ NH}-V_5 \text{ CO}$ , and  $V_2 \text{ CO}-V_7 \text{ NH}$ ) (Figure 3). The other two molecules,  $A_1$  ( $n = 2$ ) adopted a random structure and  $A_3$  ( $n = 4$ ) adopted a cyclic structure with one hydrogen bond ( $V_2 \text{ NH}-V_7 \text{ CO}$ ) (supplementary material).

In series B, molecule  $B_1$  ( $n = 2$ ) formed the four possible hydrogen bonds but not in a  $\beta$ -sheet structure (due to a  $\psi = 31^\circ$  for  $V_3$ ) (supplementary material), since  $B_2$  ( $n = 3$ ) (**2**) can form three hydrogen bonds ( $F_4 \text{ CO}-G_5 \text{ NH}$ ,  $F_4 \text{ NH}-G_5 \text{ CO}$ , and  $K_2 \text{ CO}-A_7 \text{ NH}$ ). However only the two first hydrogen bonds are formed in a  $\beta$ -sheet manner (due to a  $\psi = 37^\circ$  for  $V_3$ ) (Figure 3). Molecule  $B_3$  ( $n = 4$ ) adopted a random structure with one hydrogen bond ( $F_4 \text{ CO}-G_5 \text{ NH}$ ) (supplementary material).

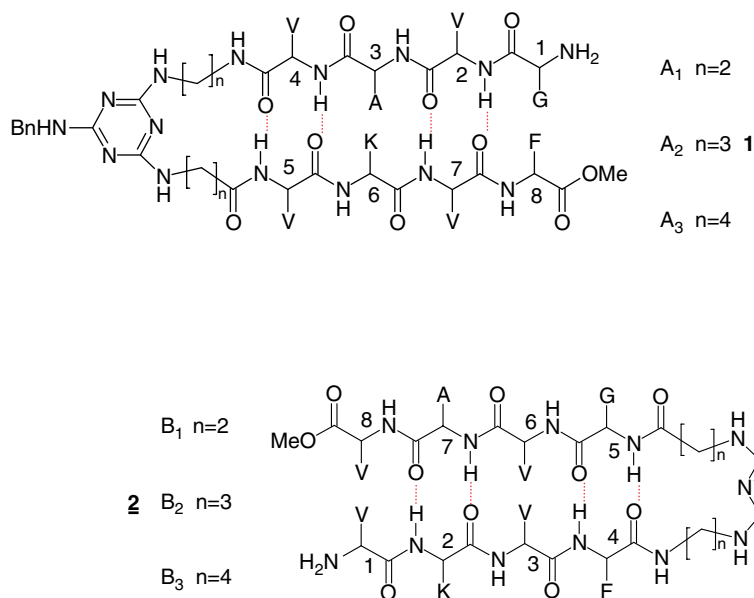


**Figure 2** Structure of molecules  $A_{1-3}$  and  $B_{1-3}$  studied by molecular modelling (potential hydrogen bonds are indicated in red).

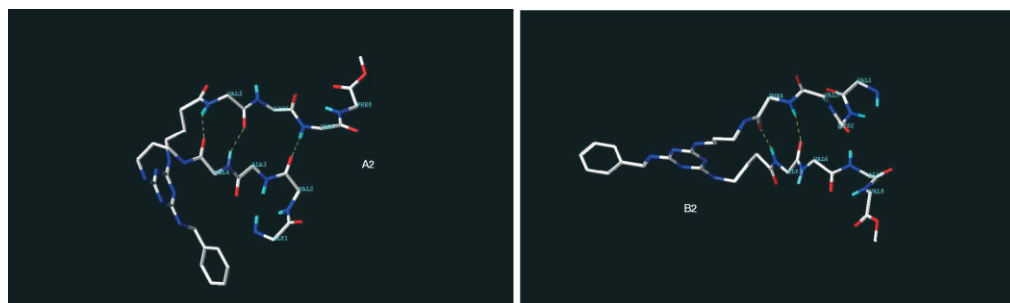


**Figure 3** Conformers of pseudopeptides **1** and **2** from MDs studies at 300 °K.

From this molecular study, we could deduce that the  $-(CH_2)_3$ -linker is the best linker and that a 17-membered ring intra-molecular hydrogen bond is ideal for nucleating  $\beta$ -sheet formation. We could also deduce that in molecule **1** which seems to adopt a  $\beta$ -sheet structure with three hydrogen bonds, the  $-(CH_2)_3$ -linkers prefer to adopt a folded conformation where the alkyl chains are oriented perpendicular to the triazine ring. These results could be compared with the results of Kelly who observed that the anti-parallel dibenzofuran and biphenyl-based templates promote a 15-membered ring and where the alkyl chains are oriented perpendicularly to the plane of the aromatic rings [29–32].

Following the results of this MDs study, we decided to synthesize both molecules **1** ( $A_2$ ) and **2** ( $B_2$ ).

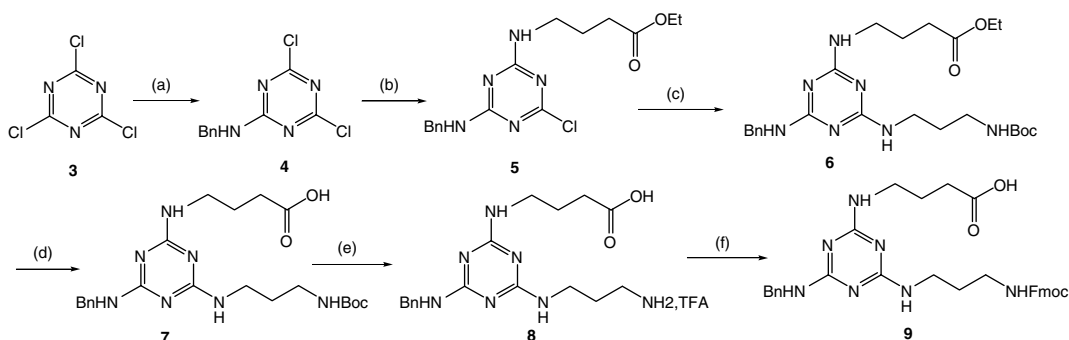
Pseudopeptides **1** and **2** containing unsymmetrical triamino 1,3,5-triazine were synthesized on solid-phase supports following a Fmoc protection strategy on Wang-Merrifield resin [57]. The unsymmetrical triamino 1,3,5-triazine scaffold **9** was synthesized in solution. As seen above, the stepwise substitution of the cyanuric chloride is well documented: it usually

requires cold temperature ( $-20$  to  $0^\circ\text{C}$ ) for substitution of the first chloride, room temperature for substitution of the second chloride, and reflux in acetonitrile or DMF/acetonitrile or THF for introduction of the final substituent [43–56]. For this purpose, addition of 1 eq. of benzylamine to cyanuric chloride **3** in dichloromethane at  $-20^\circ\text{C}$  to room temperature in the presence of 1 eq. of DIPEA afforded adduct **4** in which a single chlorine was substituted in 98% yield (Scheme 1). The subsequent reaction of compound **4** with 1.2 eq. of commercial ethyl-4-aminobutyrate at room temperature in acetonitrile led to the disubstituted adduct **5** with 90% yield. The final substituent was introduced by reaction of compound **5** with Boc-1,3-diaminopropane in refluxing acetonitrile to afford the trisubstituted product **6** with 84% yield. Saponification of the ethyl ester **6** gave the acid **7** with quantitative yield (Scheme 1). The Fmoc strategy on solid-phase chosen for the synthesis of pseudopeptides **1** and **2** led us to exchange the protecting Boc group of compound **7** by a Fmoc group. We could not directly introduce Fmoc-diaminopropane because basic cleavage of the Fmoc group would

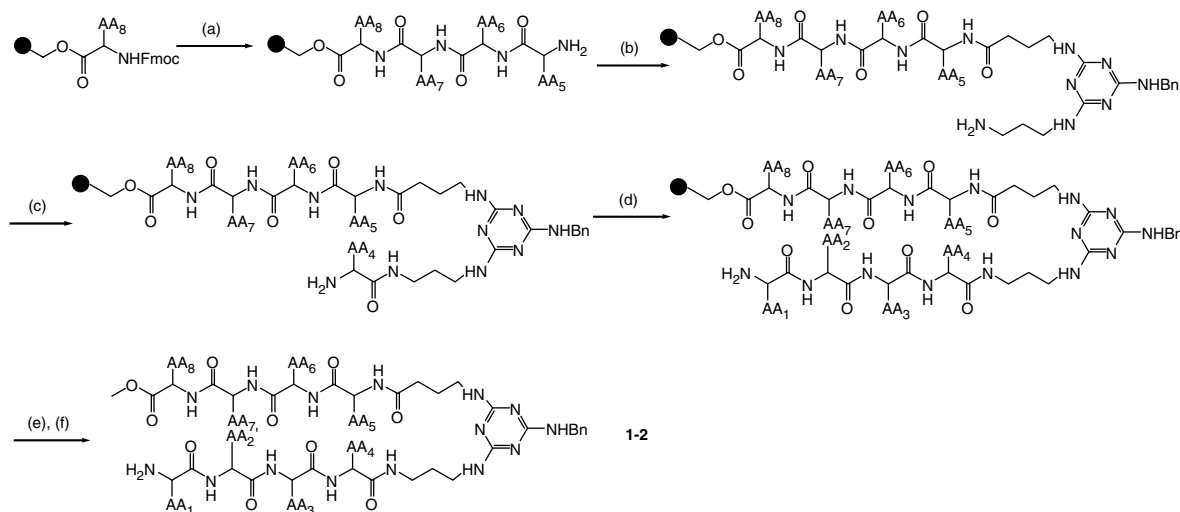
happen during the final saponification of the ethyl ester group. So, easy cleavage of the Boc group followed by re-protection of the free amino group of **8** with the Fmoc group using Fmoc-O-succinimide (FmocONSu) gave Fmoc-[triazine]-OH compound **9** in a quantitative yield (Scheme 1).

A representative sequence for solid-phase synthesis of the constrained pseudopeptides **1** and **2** is outlined in Scheme 2. Deprotection of the Fmoc-AA<sub>8</sub>-Wang-Merrifield resin was classically done with a 20% piperidine solution in DMF. Peptidic coupling between amino acids was performed with *N,N'*-Diisopropylcarbodiimide (DIC)/HOAt, with a 3.6 excess of amino acids and coupling agents, and completion of the coupling reaction was verified by performing a 2,4,6-trinitrobenzene-sulphonic acid (TNBS) [58] and a Kaiser [59] tests. In the case

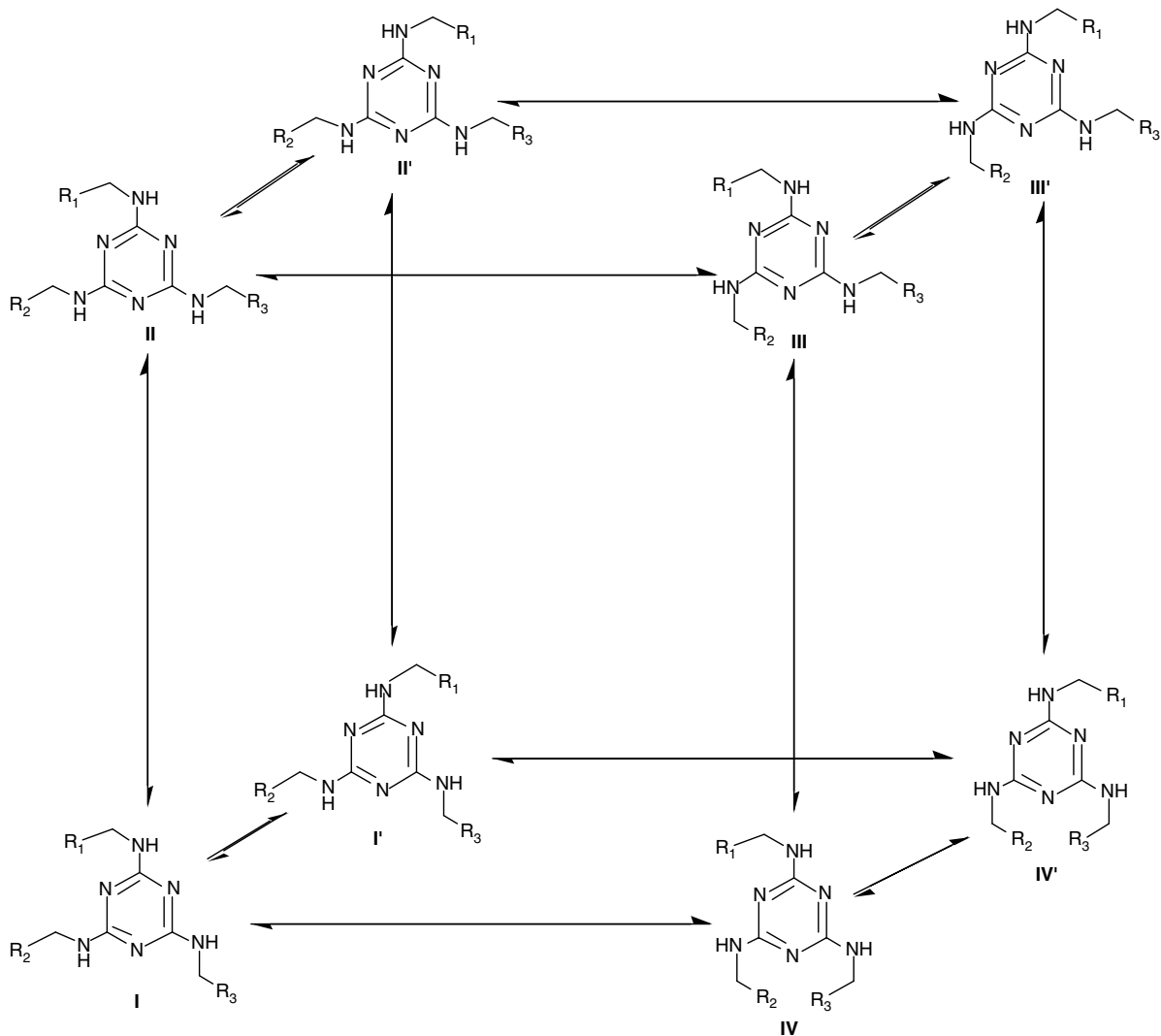
of incomplete peptide synthesis, the individual free amino groups were capped by acetylation. Then the deprotection of the amino groups occurred in the presence of a 20% piperidine solution in DMF. The conditions for the attachment of the triazine block to the growing peptide chain were HATU/HOAt/2,4,6-collidine/Fmoc-[triazine]-OH/H-AA<sub>5</sub>-AA<sub>6</sub>-AA<sub>7</sub>-AA<sub>8</sub>-O-resin in a ratio 2:2:2:1:1.2 for 15 h at room temperature. The coupling was performed with the potent Carpino's reagent HATU [60–63] which is highly efficient for the difficult coupling reactions of hindered substrates. To avoid epimerization or Fmoc *N*-deprotection which could occur with DIPEA, we used the 2,4,6-collidine as a base [64]. TNBS [58] and Kaiser *et al.* [59] tests showed that two cycles were necessary for quantitative coupling. After *N*-deprotection, incorporation of the subsequent amino acid on



**Scheme 1** Synthesis of the Fmoc-[triazine]-OH compound **9**. Reagents and conditions: (a) Benzylamine, DIPEA, CH<sub>2</sub>Cl<sub>2</sub>, –20 °C to rt, 2 h, 98%; (b) Ethyl-4-aminobutyrate hydrochloride, DIPEA, CH<sub>3</sub>CN, –10 °C to rt, 2 h, 90%; (c) Boc-1,3-diaminopropane, DIPEA, CH<sub>3</sub>CN, reflux, overnight, 84%; (d) NaOH, water/THF, reflux, 3.5 h, quantitative; (e) TFA/CH<sub>2</sub>Cl<sub>2</sub>, rt, 1 h, quantitative; (f) Na<sub>2</sub>CO<sub>3</sub> (10%), FmocONSu, THF, 0 °C, 20 min, quantitative.



**Scheme 2** General scheme for solid-phase synthesis of the constrained peptide. Reagents and conditions: (a) 20% piperidine/DMF followed by Fmoc-AA<sub>n</sub>-OH, DIC, HOAt, CH<sub>2</sub>Cl<sub>2</sub>/DMF, 2.5 h followed by Ac<sub>2</sub>O, DMAP, CH<sub>2</sub>Cl<sub>2</sub>, 2 h followed by 20% piperidine/DMF; (b) Fmoc-[triazine]-OH, HOAt, HATU, 2,4,6-collidine, CH<sub>2</sub>Cl<sub>2</sub>/DMF, 15 h followed by Ac<sub>2</sub>O, DMAP, CH<sub>2</sub>Cl<sub>2</sub>, 2 h followed by 20% piperidine/DMF; (c) Fmoc-AA<sub>4</sub>-OH, HOAt, HATU, 2,4,6-collidine, CH<sub>2</sub>Cl<sub>2</sub>/DMF, 15 h, followed by Ac<sub>2</sub>O, DMAP, CH<sub>2</sub>Cl<sub>2</sub>, 2 h followed by 20% piperidine/DMF; (d) *N*-Fmoc-AA<sub>n</sub>-OH, DIC, HOAt, CH<sub>2</sub>Cl<sub>2</sub>/DMF, 2.5 h followed by Ac<sub>2</sub>O, DMAP, CH<sub>2</sub>Cl<sub>2</sub>, 2 h followed by 20% piperidine/DMF; (e) DMF/MeOH/Et<sub>3</sub>N, reflux, 24 h; (f) HCl/MeOH, rt, 16 h.



**Scheme 3** Possible conformers of unsymmetrical triamino 1,3,5-triazine derivatives.

the H-triazazine-AA<sub>5</sub>-AA<sub>6</sub>-AA<sub>7</sub>-AA<sub>8</sub>-O-resin (1 eq.) was accomplished with an excess 4 of HATU/HOAt/2,4,6-collidine/Fmoc-AA<sub>4</sub>-OH. The coupling efficiency tests showed that one cycle was sufficient for quantitative coupling. After *N*-deprotection the coupling with the last amino acids was again performed with DIC/HOAt (with an excess 3 of amino acids and coupling agents). After a final Fmoc group cleavage, final cleavage of the peptide from the resin was performed with direct basic methanolysis by TEA/MeOH/DMF solution at reflux 24 h (two cycles). The desired compounds were separated from small peptides by flash chromatography on silica gel or by precipitation in MeOH with 20–40% overall yields. The last step consisted in the deprotection of the Lysine side chain from its Boc protective group with a solution of HCl/MeOH at room temperature.

Analysis of the structure of pseudopeptides **1** and **2** was performed by NMR spectroscopy, IR and CD. CD spectroscopy of compound **1** in H<sub>2</sub>O or in HFIP exhibited a minimum at 196 nm consistent with a

random coil conformation and a small minimum at 229 nm, consistent with a  $\beta$ -sheet conformation. CD spectroscopy of compound **2** in H<sub>2</sub>O exhibited a minimum at 196 nm and a maximum at 217 nm, consistent with a random coil conformation. CD spectroscopy of compound **2** in HFIP exhibited two minima at 196 nm (consistent with a random coil conformation) and 229 nm (consistent with a  $\beta$ -sheet conformation). IR spectroscopy of compound **1** in solid-phase exhibited a band at  $\nu = 3279\text{ cm}^{-1}$  which is characteristic of hydrogen bond N–H and also a band at  $\nu = 1631\text{ cm}^{-1}$  which is characteristic of a  $\beta$ -sheet conformation [31,32,65]. The NMR spectra of pseudopeptides **1** and **2** presented resonance overlaps and more spin systems than expected for an 8-residue peptide. The assignments were hampered by the succession of residues, in slow and/or intermediate exchange on the NMR time scale, which had very similar chemical shifts leading to broad resonances. The severe resonance overlaps prevented unambiguous

assignments of all residues in the various forms. The 2D TOCSY spectra were used to identify spin systems of each residue. The HN-H $\alpha$  region of pseudopeptide **1** reveals at least two spin systems for all amino acids and the spacer groups. Furthermore in the heteronuclear single quantum coherence (HSQC) experiment at 298°K, two cross-peaks (C $\alpha$ /H $\alpha$ ) were observed for each residue. These multiple resonances were averaged at a higher temperature, indicating that an exchange process occurred. At 298°K, two forms of pseudopeptide **1** remained in slow exchange on the NMR time scales. The cross-peaks observed between these two forms in the 2D EXSY (exchange spectroscopy) spectrum confirm the exchange between two families of resonances. The signals of the minor form of pseudopeptide **1** were sharp whereas those of the major species were broad. Thus, an intermediate exchange between different species occurred in the major form. Between 2 and 0.5 mM, no shifts were found in the <sup>1</sup>H-NMR spectra, indicating the absence of aggregate equilibrium. The tautomer equilibrium between triazine and *N*-alkylimine were also excluded on the basis of different substituted triazines as reported in literature. These types of equilibrium always shift towards triazine forms [66–68]. The strong overlaps in the pseudopeptides **1** and **2** prevent the conformational analysis around the triazine scaffold. The trisubstituted triazine **9** was analysed by NMR in the same conditions. Its 2D TOCSY spectrum showed the presence of four triplets for the H(7) amine proton and multiple peaks for the other protons, in particular for HN(15), HN(20), and HN(24) (Figure 4).

The corresponding triplets for H(7) amine proton, arising from coupling to CH<sub>2</sub>(8) were broadened at 298°K and coalesced at 333°K. The 1D spectra recorded at lower temperatures did not show extensive line broadening due to the other restricted motions. Further assignments of these different rotamers required

the use of <sup>13</sup>C and <sup>15</sup>N resonances [66–69]. The low solubility of the intermediate triazine **9** and pseudopeptides **1** and **2** prevent these types of analyses and therefore the assignments of different rotamers.

The NMR behaviour of pseudopeptides **1** and **2** was compared to the substituted triazines reported in the literature. The crystalline structures of triazine containing molecules revealed that the three exocyclic amino groups were in sp<sup>2</sup> hybridization state according to the low value of the C<sub>triazine</sub>-N<sub>exo</sub> bond length. The rotational energy barriers around C<sub>triazine</sub>-N<sub>exo</sub> bond were estimated at the coalescence temperature (298°K) to 60 KJ.mole<sup>-1</sup> for a substituted phenyl-triazine [66] and 55 KJ.mole<sup>-1</sup> (270°K) for a triazine with three butyl substituents [70]. In the crystalline structures the R<sub>1</sub>, R<sub>2</sub>, and R<sub>3</sub> groups adopted either perpendicular or parallel orientations towards the triazine plane leading to another set of conformers (Scheme 3). Their inter-conversions must be fast in the NMR time scale since they are related to the rotational energy barriers around the simple C<sub>alkyl</sub>-N<sub>exo</sub> bond. Thus, for an unsymmetrical triazine (R<sub>1</sub> ≠ R<sub>2</sub> ≠ R<sub>3</sub>) eight rotamers, can be detected by NMR. The diversities of R group location (in the triazine plane, up and down the triazine plane) lead to the unsymmetrical triazine, a scaffold where the folding and dynamics of R groups can be independent of each other. In this case, the chemical shifts should be similar in the eight rotamers leading only to resonance broadening. The presence of a unique rotamer should correspond to a strong interaction between two R substituents as expected for the formation of a  $\beta$ -sheet structure. The presence of one type of rotamer in equilibrium with other rotamers should indicate the presence of cooperative conformational effects between two of the three substituents (Scheme 3). Furthermore, if there is no interaction between the R<sub>1</sub>, R<sub>2</sub>, and R<sub>3</sub>

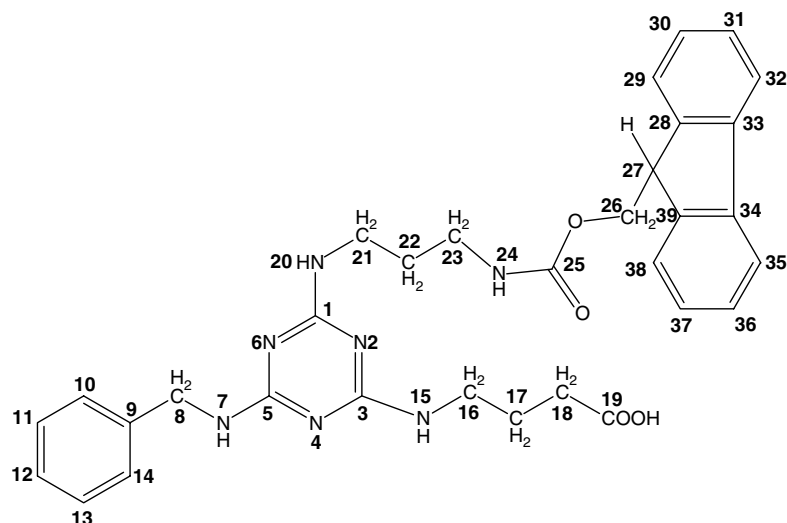


**Figure 4** Fmoc-[triazine]-OH, compound **9**.

substituents, the population of the eight rotamers should be equal.

In the pseudopeptides **1** and **2** ( $R_1 = \text{benzyl}$ ,  $R_2 = N\text{-terminal peptide}$ , and  $R_3 = C\text{-terminal domain}$ ), the I, II, III, and IV rotamers differ from I', II', III', and IV' rotamers by the benzyl group orientations. The interactions between the peptide domain and the benzyl group are probably weak. For pseudopeptides **1** and **2**, the proton chemical shifts in I, II, III, I', II', and III' rotamers must be similar to the free peptides. These rotamers constitute a set of resonances of the major form whereas the rotamers IV and IV' produced another set of resonances. In the absence of a strong interaction between the N- and C-peptide domain, the amount of rotamers IV and IV' must represent 25% of conformational equilibrium. The measurement of the cross-peak area in the TOCSY spectra of pseudopeptides **1** and **2** produced an average value of  $28 \pm 6\%$  suggesting the absence of a strong interaction between the peptide domains.

### Conformations of the Peptide Domains

**Secondary structures.** The  $H_\alpha$  and  $C_\alpha$  chemical shift deviations (CSD) depend on the secondary structure of the peptide backbone [71]. Upfield and downfield shifts of  $H_\alpha$  and  $C_\alpha$ , respectively indicate the presence of helical structure whereas upfield and downfield shifts of  $C_\alpha$  and  $H_\alpha$ , respectively signal the presence of  $\beta$ -strand. As expected, no significant deviations were observed for the major forms of pseudopeptides

**1** and **2**, demonstrating the presence of peptide random coil structures in I, II, III, I', II', and III' rotamers. However, the CSD must be corrected by primary sequences and by the presence of free amino groups, a C-terminal ester and a spacer [72]. To circumvent these corrections the difference of chemical shifts between minor and major rotamers were calculated. From these values, it is clear that the N-tripeptide  $V_2A_3V_4$  and the C-dipeptide  $V_5K_6$  of the minor form of pseudopeptide **1** adopt mainly an extended structure (rotamers IV and IV') (Table 1). The scalar coupling constants are greater than 7.3 Hz as expected for extended conformation [73]. The amplitude of  $HN/H_\alpha$  dipolar coupling constants agree also with an extended conformation since the intra-residue dipolar couplings were weaker than for adjacent residues. In conclusion, three NMR parameters agree with the formation of two  $\beta$ -strands of the N and C domain of pseudopeptide **1** as suggested by the molecular dynamic calculation.

The secondary structure analysis of pseudopeptide **2** was also based on the chemical shifts of  $H_\alpha$  and  $C_\alpha$ . The results observed for the major form(s) show again an unstructured conformation whereas the downfield shifts of  $H_\alpha$  and upfield shifts of  $C_\alpha$  resonances observed for the minor form indicate a slightly extended (Table 2) conformation propensity. However,  $H_\alpha$  shifts agree with  $\beta$ -strand in the C-terminal domain whereas the  $C_\alpha$  shifts agree with a  $\beta$ -strand in the N-terminal domain (Table 2). This discrepancy suggests the presence of another conformation in the random coil distribution.

**Table 1** NMR assignment of 2 mM pseudopeptide **1** in methanol at 298 °K. The different forms are indicated by M and m (for major and minor forms, respectively)

Residue	NH	$C_\alpha$	$H_\alpha$	$H_\beta$	Other H
Gly <sub>1</sub> (M)	NH <sub>2</sub> -	—	3.74	—	—
Gly <sub>1</sub> (m)	—	—	3.64	—	—
Val <sub>2</sub> (M)	8.32	60.14	4.26	2.09	$\gamma$ 0.96, 0.96
Val <sub>2</sub> (m)	8.47	59.95	4.42	—	—
Ala <sub>3</sub> (M)	8.36	50.32	4.41	1.33	—
Ala <sub>3</sub> (m)	8.47	49.93	4.65	—	—
Val <sub>4</sub> (M)	7.89	60.50	4.07	—	$\gamma$ 0.94, 0.94
Val <sub>4</sub> (m)	8.13	59.89	4.18	—	—
Val <sub>5</sub> (M)	7.96	60.50	4.10	2.03	$\gamma$ 0.94, 0.94
Val <sub>5</sub> (m)	8.08	60.14	4.30	—	—
Lys <sub>6</sub> (M)	8.22	54.19	4.38	1.83, 1.77	$\gamma$ 1.39; $\delta$ 1.63; $\epsilon$ 2.88; NH <sub>2</sub> 7.74
Lys <sub>6</sub> (m)	8.43	53.94	4.51	—	—
Val <sub>7</sub> (M)	7.92	59.89	4.18	2.03	$\gamma$ 0.94, 0.94
Val <sub>7</sub> (m)	8.20	59.89	4.32	—	—
Phe <sub>8</sub> (M)	8.50	55.30	4.63	3.13, 3.01	$\delta$ 7.24; $\epsilon$ 7.24; $\zeta$ 7.24
Phe <sub>8</sub> (m)	8.54	55.30	4.70	—	—
tNH-CH <sub>2</sub> -CH <sub>2</sub> -CH <sub>2</sub> -NH (M)	—	—	—	—	8.08-3.25-1.76-3.40-8.01
tNH-CH <sub>2</sub> -CH <sub>2</sub> -CH <sub>2</sub> -NH (m)	—	—	—	—	8.22
tNH-CH <sub>2</sub> -CH <sub>2</sub> -CH <sub>2</sub> -CO	—	—	—	—	8.00-3.42-1.87-2.33
tNH-CH <sub>2</sub> -Phenyl	—	—	—	—	8.40-4.60-7.24

**Table 2** NMR assignment of 4 mm pseudopeptide **2** in methanol at 298 °K. The different forms are indicated by M and m (for major and minor forms, respectively)

Residue	NH	C $_{\alpha}$	H $_{\alpha}$	H $_{\beta}$	Other H
Val <sub>1</sub> (M)	NH <sub>2</sub>	59.89	3.71	—	$\gamma$ 1.03, 1.00
Val <sub>1</sub> (m)	—	59.89	3.76	—	
Lys <sub>2</sub> (M)	8.51	54.84	4.44	1.76, 1.67	$\gamma$ 1.38, 1.43; $\delta$ 1.66; $\epsilon$ 2.89; NH <sub>2</sub> 7.97
Lys <sub>2</sub> (m)	8.51	54.69	4.52		
Val <sub>3</sub> (M)	8.06	60.50	4.16	1.99	$\gamma$ 0.88, 0.88
Val <sub>3</sub> (m)	8.16	60.17	4.16		
Phe <sub>4</sub> (M)	8.29	56.63	4.52	3.09, 2.94	$\delta$ 7.21; $\epsilon$ 7.27; $\zeta$ 7.27
Phe <sub>4</sub> (m)	8.42	56.63	4.57		
Gly <sub>5</sub> (M)	8.30	43.84	3.90		
Gly <sub>5</sub> (m)	8.27	43.84	4.02		
Val <sub>6</sub> (M)	8.05	60.50	4.21	2.08	$\gamma$ 0.94, 0.94
Val <sub>6</sub> (m)	8.03	60.50	4.33		
Ala <sub>7</sub> (M)	8.29	50.47	4.44	1.34	
Ala <sub>7</sub> (m)	8.41	50.47	4.54		
Val <sub>8</sub> (M)	8.15	59.56	4.29	2.08	$\gamma$ 0.93, 0.93 OCH <sub>3</sub> 3.69
Val <sub>8</sub> (m)	8.28	59.56	4.29		
tNH-CH <sub>2</sub> -CH <sub>2</sub> -CH <sub>2</sub> -NH (M)	—	—	—	—	7.81-3.26-1.67-3.18-8.03
(m)	—	—	—	—	7.73/7.58-3.26-1.69/1.59-3.18-7.94
tNH-CH <sub>2</sub> -CH <sub>2</sub> -CH <sub>2</sub> -CO (M)	—	—	—	—	7.86-3.43-1.88-2.34
(m)	—	—	—	—	7.85/7.81/7.68-3.43-1.91-2.34
tNH-CH <sub>2</sub> -Phenyl (M)	—	—	—	—	8.03-4.58-7.31-7.27
(m)	—	—	—	—	7.32

The differences of CSD between the two minor forms of pseudopeptides **1** and **2** demonstrate that the  $\beta$ -strand conformation is quantitatively less significant for pseudopeptide **2** than for pseudopeptide **1**.

**Ternary structures.** In the pseudopeptide **1**, the temperature coefficients of the amide protons remain between  $-8$  and  $-10$  ppb/K demonstrating the lack of strong intra-molecular hydrogen bonds between the two  $\beta$ -strands. The more positive values of the residue Val<sub>5</sub> and Phe<sub>8</sub> suggest the formation of transient intra-molecular hydrogen bonds during the backbone dynamic. The overlap resonances in the pseudopeptide **2** do not allow for the determination of temperature coefficients of the amide protons. In the ROESY spectra of pseudopeptides **1** and **2**, no dipolar coupling constants were observed between the  $\beta$ -strands. Thus in methanol, these two  $\beta$ -strands do not form a  $\beta$ -sheet as expected from the MDs calculation using a weak dielectric constant.

**These structural data raise two questions.** What are the driving forces of  $\beta$ -strand formation? Why do two  $\beta$ -strands attached to a mimic  $\beta$ -turn scaffold not form a stable  $\beta$ -sheet? To answer these questions, we must consider that generally the conformational space of an amino acid located in I position depends on the side chain volumes of  $i$ ,  $i+1$ , and  $i-1$  residues and on the backbone solvation. In the case of disubstituted triazine, the conformational space of

one amino acid located in the R<sub>1</sub> arm depends on the conformational space of amino acids of R<sub>3</sub> arm. These restrictions of conformational spaces favour the extended conformation. In the pseudopeptide **2**, the presence of Gly increases the conformational space on both arms leading to a decrease of  $\beta$ -strands. The trend is probably independent of solvation.

The formation of a  $\beta$ -sheet depends on the strengths of the hydrogen bond and side chain interactions between the two  $\beta$ -strands, which are favoured by hydrophobic and polar media, respectively. Methanol favours the  $\alpha$ -helix [74] structure by modulating the exposure of hydrophobic and hydrophilic atoms of the peptide. The maximal intra-molecular hydrogen bonds correspond generally to the  $\alpha$ -helix. However, if the conformational energy of  $\beta$ -sheet structure is significantly lower than that of  $\alpha$ -helix, alcohol may induce  $\beta$ -sheet structure. The triazine scaffold and methanol prevent the formation of the helix structure and intra-molecular hydrophobic interaction between side chains, respectively. To overcome the solvation effect, new triazine derivatives must be developed to perform the study in water.

## CONCLUSIONS

We synthesized on solid-phase the unsymmetrical pseudopeptides **1** and **2** incorporating a triazine scaffold. Conformational studies were performed by



NMR spectroscopy. The scaffold was based on triamino 1,3,5-triazine bearing two alkyl chains where  $n = 3$  proved to be a mimic of the backbone of the  $i + 1$  and  $i + 2$  residues of a  $\beta$ -turn by reversing the polypeptide chain direction. This triazine scaffold proved also to be an inducer of extended conformations and therefore it is a good candidate as a template to induce anti-parallel structure. Also predicted by molecular modelling, pseudopeptide **1** which contains the series  $G_1V_2A_3V_4$  and  $V_5K_6V_7F_8$  possesses a  $\beta$ -strand conformation quantitatively greater than for pseudopeptide **2** which contains the opposite series  $V_1K_2V_3F_4$  and  $G_5V_6A_7V_8$ . So the triazine:peptide chimer represents a valuable tool to analyse independently the  $\beta$ -strand and  $\beta$ -sheet formations and to estimate the energy of ternary structure stabilization by measuring the percentage of the triazine rotamers. Further studies on triazine molecules will include, in particular, the following:

- (i) The synthesis of new unsymmetrical triamino 1,3,5-triazine derivatives in order to stabilize  $\beta$ -sheet structure by (a) modifying the peptidic arms by changing amino acids (hydrophobic or charged amino acids) or using peptidomimetics; (b) testing more than four amino acids on each of the peptidic arms; (c) performing studies in water and by this way, displacing the equilibrium of the conformers to the IV or IV' rotamers (Scheme 3) which are favorable to induce  $\beta$ -sheet structuration
- (ii) Screening of these triazine molecules as  $\beta$ -sheet ligands and testing their eventual ability to prevent aggregation of Alzheimer's peptide A $\beta$  (1–40) and of the prion protein.

## EXPERIMENTAL

### General Chemical Techniques

The usual solvents were purchased from commercial sources and dried and distilled by standard procedures. The FmocVal 4-benzyloxybenzyl ester polymer bound Wang-Merrifield and the FmocPhe 4-benzyloxybenzyl ester polymer bound Wang-Merrifield resins were purchased from Fluka (0.4–0.6 mmol/g resin). Cyanuric chloride, benzylamine, ethyl-4-aminobutyrate hydrochloride, Fmoc-AA<sub>n</sub>-OH, DIC, HOAt, and HATU were purchased from commercial sources. Boc-1,3-diaminopropane was prepared according to literature procedure [75]. Pure products were obtained after flash chromatography using Merck silica gel 60 (40–63  $\mu$ m). TLC analyses were performed with 0.25-mm 60 F<sub>254</sub> silica plates (Merck). Element analyses (C, H, N) were performed on a Perkin-Elmer CHN, Analyser 2400. Mass spectra were obtained using a Bruker Esquire electrospray ionization apparatus. IR spectra were recorded on a Bruker Vector 22 FT-IR spectrometer. NMR spectra were recorded on a Bruker AMX 200, (<sup>1</sup>H, 200 MHz, <sup>13</sup>C, 50 MHz) or Bruker AVANCE 400 (<sup>1</sup>H, 400 MHz, <sup>13</sup>C, 100 MHz). Chemical shift  $\delta$  are in ppm and the following abbreviations are used: singlet (s), doublet (d), triplet (t), multiplet (m), quintet (q),

broad singlet (bs), and broad doublet (bd). A preparative HPLC was carried out on a dual pump system equipped with Thermo spectra SYSTEM solvent helium module P1000XR. The column employed was a Thermo ODS Hypersil (250  $\times$  10 mm, 5  $\mu$ m) attached to a spectra SERIES UV 100 detector set at 220 nm. Solvent A was composed of water and 0.1% TFA. Solvent B was composed of 60% CH<sub>3</sub>CN, 40% water, and 0.1% TFA. Far- and near-UV CD spectra were recorded on a Jobin Yvon CD6 spectrometer at 25 °C using a 1-mm quartz cell between 185 and 340 nm using an integration time of 1 s, an increment of 0.5 nm, a band width of 2 nm and a constant bandpass of 2 nm.

### Material and Methods for NMR Study

NMR samples were prepared in methanol (CD<sub>3</sub>OH) at 2- and 4-mM concentrations. The NMR spectra were recorded on a Bruker DRX 500 spectrometer and were processed with the Bruker UXNMR software. 1D spectra were acquired over 32 K data points using a spectral width of 5000 Hz. Solvent suppression was achieved by pre-saturating during the relaxation delay (2 s). 2D experiments were acquired in absolute mode for COSY and in phase mode for TOCSY [76] and ROESY experiments [77] using time proportional phase incrementation [78], with the transmitter set on the residual solvent signal. <sup>1</sup>H-<sup>13</sup>C HSQC experiments were recorded using gradient pulses for coherence selection [79]. TOCSY experiments were carried out with a mixing time  $\tau_m$  equal to 70 ms. ROESY spectra were obtained at 200 and 500 ms mixing times. Typically, 512 increments were acquired over a spectral width of 5000 Hz. Prior to Fourier transformation in  $t_2$  and  $t_1$  dimensions, the free induction decays were zero-filled and multiplied by a  $\pi/2$ -shifted sinebell function. The <sup>1</sup>H-NMR spectra of the peptides have been completely assigned from COSY, TOCSY, and ROESY spectra [80]. The <sup>13</sup>C-NMR spectra have been partially assigned from HSQC spectra. The resonance assignments are listed in Tables 1 and 2. The chemical shift deviations are calculated as the differences between observed chemical shifts and random coil values. The random coil values of amide and H <sub>$\alpha$</sub>  protons were determined in methanol [81]. The C <sub>$\alpha$</sub>  chemical shift deviation was calculated using random coil values reported in water [82]. The temperature gradients of the amide proton chemical shifts were derived from 1D, 2D TOCSY, and ROESY spectra recorded at 278, 285, 291, 298, and 303 °K. The methyl protons of methanol provided a reference since they did not change their chemical shifts at various temperatures. <sup>3</sup>J coupling constants were extracted from 1D spectrum at 298 °K.

### N-Benzyl-4,6-Dichloro-1,3,5-Triazin-2-Amine (4)

A stirred solution of cyanuric chloride (3.52 g, 19 mmol) in CH<sub>2</sub>Cl<sub>2</sub> (176 ml) was cooled to -20 °C. A solution of benzylamine (2.07 ml, 19 mmol, 1 equiv.) and DIPEA (3.3 ml, 19 mmol, 1 equiv.) in CH<sub>2</sub>Cl<sub>2</sub> (21 ml) was then added dropwise over a period of 30 min to the cyanuric chloride solution. The resulting mixture was allowed to warm to room temperature and stirred for 2 h. The reaction mixture was cooled to 0 °C and quenched by pouring it into a 5% aqueous citric acid solution (141 ml) and extracting with CH<sub>2</sub>Cl<sub>2</sub> (3  $\times$  200 ml). The organic layers were combined,

dried over Na<sub>2</sub>SO<sub>4</sub>, filtered, and concentrated *in vacuo*. Recrystallization of the crude product in MeOH afforded the monosubstituted dichlorotriazine **4** (4.74 g, 98%) as a white solid. *R*<sub>f</sub> = 0.60 (cyclohexane/EtOAc 5:5); m.p. 120–122 °C (lit.: 116–118 °C [83]); <sup>1</sup>H NMR (200 MHz, DMSO-*d*<sub>6</sub>, 25 °C): δ = 9.69 (t, <sup>3</sup>*J*(H,H) = 6 Hz, 1H, NH), 7.40–7.30 (m, 5 H, aromatic H), 4.62 (d, <sup>3</sup>*J*(H,H) = 6 Hz, 2H, CH<sub>2</sub>-Ph); <sup>13</sup>C NMR (50 MHz, DMSO-*d*<sub>6</sub>, 25 °C): δ = 169.8, 169.0, 165.8, 137.8, 128.7, 128.5, 127.6, 127.5, 127.0, 44.3; IR (neat): ν = 3255 (NH), 846 (C–Cl), 797 (C–Cl) cm<sup>-1</sup>; C<sub>10</sub>H<sub>8</sub>Cl<sub>2</sub>N<sub>4</sub> (255.10): calcd C, 47.08; H, 3.16; N 21.96; found C, 46.91; H, 3.90; N, 21.85.

#### Ethyl 4-(4-(Benzylamino)-6-Chloro-1,3,5-Triazin-2-Ylamino)Butanoate (5)

A stirred solution of monosubstituted triazine intermediate **4** (1 g, 3.9 mmol) in CH<sub>3</sub>CN (15 ml) was cooled to -10 °C. A solution of DIPEA (2.04 ml, 11.7 mmol, 3 equiv.) and ethyl-4-aminobutyrate hydrochloride (788 mg, 4.7 mmol, 1.2 equiv.) in CH<sub>3</sub>CN (25 ml) was added dropwise. The resulting mixture was stirred at 0 °C for 5 min after addition was complete and then allowed to warm to room temperature and stirred for 2 h. The reaction mixture was then poured into water (10 ml) and extracted with EtOAc (3 × 50 ml). The organic layers were combined, then washed with a 5% aqueous citric acid solution (10 ml) and brine (10 ml), dried over Na<sub>2</sub>SO<sub>4</sub>. Filtration and concentration *in vacuo* gave a pale yellow solid which was recrystallized in EtOAc/cyclohexane to afford the disubstituted monochlorotriazine **5** (1.22 g, 90%) as a white solid. *R*<sub>f</sub> = 0.40 (cyclohexane/EtOAc 5:5); m.p. 165–167 °C; <sup>1</sup>H NMR (200 MHz, CDCl<sub>3</sub>, 25 °C): δ = 7.12–7.02 (m, 6H, aromatic H, NH), 6.61 (t, <sup>3</sup>*J*(H,H) = 6 Hz, 1H, NH), 4.45 (d, <sup>3</sup>*J*(H,H) = 6 Hz, 2H, CH<sub>2</sub>-Ph), 3.91 (q, <sup>3</sup>*J*(H,H) = 7 Hz, 2H, CH<sub>2</sub>-CH<sub>3</sub>), 3.27–3.20 (m, 2H, CH<sub>2</sub>-NH), 2.19–2.06 (m, 2H, CH<sub>2</sub>-COEt), 1.70–1.63 (m, 2H, -CH<sub>2</sub>-), 1.04 (t, <sup>3</sup>*J*(H, H) = 7 Hz, 3H, CH<sub>3</sub>); <sup>13</sup>C NMR (50 MHz, CDCl<sub>3</sub>, 25 °C): δ = 172.9, 167.8, 165.6, 138.4, 128.4, 127.5, 127.1, 60.3, 44.6, 40.1, 31.4, 24.5, 14.0; IR (neat): ν = 3250 (NH), 3112 (NH), 1729 (C=O), 1096 (C–O), 797 (C–Cl) cm<sup>-1</sup>; C<sub>16</sub>H<sub>20</sub>ClN<sub>5</sub>O<sub>2</sub> (349.82): calcd C, 54.94; H, 5.76; N, 20.02; found: C, 55.15; H, 5.93; N, 19.91; MS (ESI, ion polarity positive): *m/z*: 350.2 [M<sup>+</sup> + H], 372.1 [M<sup>+</sup> + Na].

#### Ethyl 4-(6-(Benzylamino)-4-(3-*tert*-Butoxycarbonylaminopropylamino)-1,3,5-Triazin-2-Ylamino)Butanoate (6)

To a stirred solution of disubstituted monochlorotriazine **5** (1.6 g, 4.5 mmol) in CH<sub>3</sub>CN (17 ml), a solution of DIPEA (1.03 ml, 5.9 mmol, 1.3 equiv.) and Boc-1,3-diaminopropane (1 g, 5.9 mmol, 1.3 equiv.) was added dropwise in CH<sub>3</sub>CN (34 ml) at room temperature. The resulting mixture was stirred at room temperature for 5 min and then allowed to warm to reflux and stirred overnight. The reaction mixture was cooled to room temperature, then poured into a 5% aqueous citric acid solution (15 ml), extracted with EtOAc (3 × 50 ml). The organic layers were combined, then washed with brine (10 ml), dried over Na<sub>2</sub>SO<sub>4</sub> and concentrated *in vacuo*. After purification by flash column chromatography on silica gel of the residue (cyclohexane/EtOAc, 5:5, then EtOAc and EtOAc/MeOH, 95:5), the triazine analogue intermediate **6**

(1.83 g, 84%) was obtained as a yellow oil. *R*<sub>f</sub> = 0.25 (cyclohexane/EtOAc 6:4); <sup>1</sup>H NMR (200 MHz, CDCl<sub>3</sub>, 25 °C): δ = 7.42 (bs, 7H, aromatic H, NH), 7.06 (bs, 1H, NH), 4.69 (bs, 2H, CH<sub>2</sub>-Ph), 4.25 (q, <sup>3</sup>*J*(H,H) = 7 Hz, 2H, CH<sub>2</sub>-CH<sub>3</sub>), 3.53 (bs, 4H, 2 CH<sub>2</sub>-NH), 3.27 (bd, 2H, CH<sub>2</sub>-NH), 2.48–2.45 (m, 2H, CH<sub>2</sub>-COEt), 2.03–2.00 (m, 2H, -CH<sub>2</sub>-), 1.85–1.80 (m, 2H, -CH<sub>2</sub>-), 1.56 (s, 9H, Boc), 1.37 (t, <sup>3</sup>*J*(H, H) = 7 Hz, 3H, CH<sub>3</sub>); <sup>13</sup>C NMR (50 MHz, CDCl<sub>3</sub>, 25 °C): δ = 173.0, 156.1, 138.2, 128.3, 127.3, 127.1, 78.8, 60.2, 44.5, 39.9, 37.5, 37.1, 31.3, 29.6, 28.2, 24.5, 14.0; IR (neat): ν = 3380 (NH), 1698 (C=O), 1163 (C–O) cm<sup>-1</sup>; C<sub>24</sub>H<sub>37</sub>N<sub>7</sub>O<sub>4</sub>·1.5 H<sub>2</sub>O (487.60): calcd C, 56.01; H, 7.85; N, 19.06; found: C, 56.48; H, 7.58; N, 18.43; MS (ESI, ion polarity positive): *m/z*: 488.8 [M<sup>+</sup> + H], 975.5 [2M<sup>+</sup>].

#### 4-(6-(Benzylamino)-4-(3-*tert*-Butoxycarbonylaminopropylamino)-1,3,5-Triazin-2-Ylamino) Butanoic Acid (7)

The triazine analogue intermediate **6** (1.44 g, 2.9 mmol) was dissolved in THF (44 ml), then water (12.5 ml) and an aqueous NaOH solution (1 N) (14.7 ml, 5 equiv.) were added. The mixture was heated at reflux for 3.5 h and then concentrated *in vacuo*. The aqueous phase was acidified to pH 1 with an aqueous solution of 1 N HCl, then was extracted with EtOAc (3 × 50 ml). The extracts were washed with brine (10 ml) and dried with Na<sub>2</sub>SO<sub>4</sub>. Filtration and concentration *in vacuo* afforded compound **7** (1.34 g, quantitative) as a white foam. *R*<sub>f</sub> = 0.15 (EtOAc/MeOH 9:1); <sup>1</sup>H NMR (200 MHz, CDCl<sub>3</sub>, 25 °C): δ = 9.32 (bs, 1H, COOH), 7.11 (bs, 5H, aromatic H), 4.38 (bd, 2H, CH<sub>2</sub>-Ph), 3.24 (m, 4H, 2 CH<sub>2</sub>-NH), 2.96 (m, 2H, CH<sub>2</sub>-NH), 2.17–2.15 (m, 2H, CH<sub>2</sub>-CO), 1.71–1.68 (m, 2H, -CH<sub>2</sub>-), 1.54–1.51 (m, 2H, -CH<sub>2</sub>-), 1.23 (s, 9H, Boc); <sup>13</sup>C NMR (50 MHz, CDCl<sub>3</sub>, 25 °C): δ = 177.8, 163.1, 163.0, 156.4, 137.5, 128.4, 127.4, 79.3, 45.1, 40.4, 37.9, 32.1, 29.5, 28.2, 24.7; IR (neat): ν = 3250 (NH), 3064 (OH), 1692 (C=O), 1620 (C=O), 1043 (C–O) cm<sup>-1</sup>; C<sub>22</sub>H<sub>33</sub>N<sub>7</sub>O<sub>4</sub>·2.5 H<sub>2</sub>O: calcd C, 52.36; H, 7.61; N, 19.44; found: C, 52.52; H, 7.30; N, 18.14; MS (ESI, ion polarity positive): *m/z*: 460.2 [M<sup>+</sup> + H], 919.4 [2M<sup>+</sup>].

#### 4-(4-(3-Aminopropylamino)-6-(Benzylamino)-1,3,5-Triazin-2-Ylamino) Butanoic Acid (8)

A solution of acid **7** (1.3 g, 2.8 mmol) in CH<sub>2</sub>Cl<sub>2</sub> (42 ml) and trifluoroacetic acid (17.6 ml) was stirred for 1 h at room temperature and then concentrated *in vacuo* to afford compound **8** (1.3 g, quantitative) as an orange oil. *R*<sub>f</sub> = 0.10 (EtOAc/MeOH 9:1); <sup>1</sup>H NMR (200 MHz, MeOD, 25 °C): δ = 7.46 (bs, 5H, aromatic H), 4.73 (bd, 2H, CH<sub>2</sub>-Ph), 3.77–3.47 (m, 4H, 2 CH<sub>2</sub>-NH), 3.16–3.10 (m, 2H, CH<sub>2</sub>-NH), 2.50–2.47 (m, 2H, CH<sub>2</sub>-CO), 2.10–2.00 (m, 4H, 2 -CH<sub>2</sub>-); <sup>13</sup>C NMR (50 MHz, MeOD, 25 °C): δ = 175.4, 155.8, 155.2, 154.8, 137.3, 128.1, 127.1, 127.0, 43.5, 39.7, 37.0, 36.6, 30.5, 26.7, 23.8; IR (neat): ν = 3064 (OH), 1713 (C=O), 1043 (C–O) cm<sup>-1</sup>; MS (ESI, ion polarity positive): *m/z*: 360.2 [M<sup>+</sup> + H], 719.3 [2M<sup>+</sup>].

#### 4-(6-(Benzylamino)-4-(3-(9-Fluorenylmethoxycarbonyl) Aminopropylamino)-1,3,5-Triazin-2-Ylamino) Butanoic Acid (9)

Compound **8** (190 mg, 0.4 mmol) was dissolved in 10% Na<sub>2</sub>CO<sub>3</sub> solution (2 ml) and cooled in an ice bath. A solution

of FmocONSu (135 mg, 0.4 mmol) in THF (2 ml) was added in one portion at 0°C. The resulting mixture was stirred at 0°C for 25 min and then allowed to warm to room temperature and stirred for 10 min. The mixture was diluted with water; then the aqueous phase was acidified to pH 1 with an aqueous solution of HCl (1 N). The resulting solution was extracted with EtOAc (3 × 50 ml). The extracts were washed with brine (10 ml), dried with Na<sub>2</sub>SO<sub>4</sub>, and evaporated *in vacuo*. After purification of the residue by flash column chromatography on silica gel (cyclohexane/EtOAc, 5:5, then EtOAc and EtOAc/MeOH, 9:1), compound **9** (245 mg, quantitative) was obtained as a white solid. *R*<sub>f</sub> = 0.25 (EtOAc/MeOH 9:1); <sup>1</sup>H NMR (400 MHz, DMSO-*d*<sub>6</sub>, 80°C): δ = 8.25 (bs, 1H, *NH*Bn), 7.84 (bs, 1H, *NH*-CH<sub>2</sub>), 7.82 (bs, 1H, *NH*-CH<sub>2</sub>), 7.82 (d, <sup>3</sup>*J*(H,H) = 7 Hz, 2H, aromatic H Fmoc), 7.63 (d, <sup>3</sup>*J*(H,H) = 7 Hz, 2H, aromatic H Fmoc), 7.39–7.22 (m, 9H, aromatic H), 6.95 (bs, 1H, *NH*-CO), 4.50 (d, <sup>3</sup>*J*(H,H) = 5 Hz, 2H, CH<sub>2</sub>-Ph), 4.30 (d, <sup>3</sup>*J*(H,H) = 6 Hz, 2H, CH<sub>2</sub>-Fmoc), 4.18 (t, <sup>3</sup>*J*(H,H) = 6 Hz, 1H, CH-Fmoc), 3.31–3.30 (m, 4H, 2 CH<sub>2</sub>-NH), 3.04–3.03 (m, 2H, CH<sub>2</sub>-NH), 2.26–2.22 (m, 2H, CH<sub>2</sub>-CO), 1.79–1.72 (m, 2H, -CH<sub>2</sub>-), 1.65 (m, 2H, -CH<sub>2</sub>-); <sup>13</sup>C NMR (100 MHz, DMSO-*d*<sub>6</sub>, 80°C): δ = 179.2, 156.6, 143.8, 141.1, 137.7, 128.4, 127.5, 127.3, 126.9, 124.9, 119.8, 66.4, 47.1, 44.9, 40.5, 37.8, 33.2, 29.5, 28.9, 24.3; IR (neat): ν = 3311 (NH), 1708 (C=O), 1077 (C-O) cm<sup>-1</sup>; MS (ESI, ion polarity positive): *m/z*: 582.4 [M<sup>+</sup> + H], 1163.5 [2M<sup>+</sup>]. HRMS (EI): calcd for C<sub>32</sub>H<sub>35</sub>N<sub>7</sub>O<sub>4</sub> (582.2829), found (582.2869).

### General Procedure: H-AA<sub>1</sub>-AA<sub>2</sub>-AA<sub>3</sub>-AA<sub>4</sub>-(Triazine)-AA<sub>5</sub>-AA<sub>6</sub>-AA<sub>7</sub>-AA<sub>8</sub>-O-Wang-Merrifield Resin

A solid-phase reaction vessel was charged with Fmoc-AA<sub>8</sub>-O-Wang-Merrifield resin (1.2 equiv.), and the resin was treated with a 20% piperidine/DMF solution (10 ml/1 g of resin), 3 × 15 min, and washed with DMF (3 × 10 ml) and CH<sub>2</sub>Cl<sub>2</sub> (3 × 10 ml). Fmoc-AA<sub>7</sub>-OH (3.6 equiv.) and HOAt (3.6 equiv.) were dissolved in an anhydrous mixture of CH<sub>2</sub>Cl<sub>2</sub>/DMF, 4:1, (10 ml) under nitrogen. At 0°C, DIC (3.6 equiv.) was added dropwise to this solution. The resulting mixture was stirred for 10 min at this temperature and for another 10 min at room temperature, then added to the aforementioned H-AA<sub>8</sub>-O-Wang-Merrifield resin. This mixture was shaken at room temperature for 3.5 h, then filtered, and the resin was rinsed with DMF (3 × 10 ml) and CH<sub>2</sub>Cl<sub>2</sub> (3 × 10 ml). The coupling was assessed by performing TNBS and Kaiser tests, which showed that one cycle was sufficient for almost quantitative coupling in all cases. The free amino groups were acetylated with a solution of acetic anhydride (2 equiv.), DMAP (1 equiv.), and CH<sub>2</sub>Cl<sub>2</sub> (10 ml) at rt for 2 h. The resin was washed with DMF (3 × 10 ml) and CH<sub>2</sub>Cl<sub>2</sub> (3 × 10 ml) and the acetylation was assessed by performing TNBS and Kaiser tests. The same procedure (Fmoc cleavage, coupling step, and acetylation) was conducted to obtain Fmoc-AA<sub>5</sub>-AA<sub>6</sub>-AA<sub>7</sub>-AA<sub>8</sub>-O-Wang-Merrifield resin. A 20% piperidine/DMF solution was then used to deprotect the Fmoc group (same procedure as above). Then, HATU (2 equiv.), HOAt (2 equiv.), the corresponding Fmoc-[triazine]-OH **9** (1 equiv.), CH<sub>2</sub>Cl<sub>2</sub>/DMF (1:3, 12 ml), and 2,4,6-collidine (2 equiv.) were successively added and the mixture was shaken for 15 h at room temperature. The solution was drained and the resin was washed with DMF (3 × 10 ml) and CH<sub>2</sub>Cl<sub>2</sub> (3 × 10 ml). TNBS and Kaiser tests implicated that the capping was

incomplete and a second cycle was carried out for 2.5 h. The unreacted amino groups were acetylated as mentioned above. The solution was drained and the resin was washed with DMF (3 × 10 ml) and CH<sub>2</sub>Cl<sub>2</sub> (3 × 10 ml).

After deprotection of the Fmoc group following the usual procedure, Fmoc-AA<sub>5</sub>-OH (4 equiv.), HATU (4 equiv.), HOAt (4 equiv.), CH<sub>2</sub>Cl<sub>2</sub>/DMF (1:3, 12 ml), and 2,4,6-collidine (4 equiv.) were successively added and the mixture was shaken at room temperature for 15 h. The solution was drained and the resin was rinsed with DMF (3 × 10 ml) and CH<sub>2</sub>Cl<sub>2</sub> (3 × 10 ml). TNBS and Kaiser tests showed that one cycle was sufficient for an almost quantitative coupling. The unreacted amino groups, possibly present, were acetylated. The resin was filtered and washed with DMF (3 × 10 ml) and CH<sub>2</sub>Cl<sub>2</sub> (3 × 10 ml).

The Fmoc group was again deprotected and a solution of Fmoc-AA<sub>6</sub>-OH (3 equiv.) in CH<sub>2</sub>Cl<sub>2</sub>/DMF (4:1, 10 ml) pre-activated with DIC (3 equiv.) and HOAt (3 equiv.) in the same manner as described above, was then added and the suspension was shaken for 3.5 h at room temperature. The solution was then drained and the resin was rinsed with DMF (3 × 10 ml) and CH<sub>2</sub>Cl<sub>2</sub> (3 × 10 ml). In all cases, TNBS and Kaiser tests showed that one coupling cycle was sufficient for completion of the reaction. The resulting free amino groups were acetylated with a solution of acetic anhydride (2 equiv.), DMAP (1 equiv.), and CH<sub>2</sub>Cl<sub>2</sub> (10 ml). The resulting mixture was shaken for another 2 h at room temperature. The resin was washed with DMF (3 × 10 ml) and CH<sub>2</sub>Cl<sub>2</sub> (3 × 10 ml) and the acetylation was assessed by performing TNBS and Kaiser tests. The same procedure (Fmoc cleavage, coupling and acetylation) was conducted to obtain H-AA<sub>1</sub>-AA<sub>2</sub>-AA<sub>3</sub>-AA<sub>4</sub>-[Triazine]-AA<sub>5</sub>-AA<sub>6</sub>-AA<sub>7</sub>-AA<sub>8</sub>-O-Wang-Merrifield resin.

### Cleavage of the Peptide Mimic from the Resin (Basic Cleavage) H-AA<sub>1</sub>-AA<sub>2</sub>-AA<sub>3</sub>-AA<sub>4</sub>-(Triazine)-AA<sub>5</sub>-AA<sub>6</sub>-AA<sub>7</sub>-AA<sub>8</sub>-OMe

The resin was treated with anhydrous TEA/MeOH/DMF solution (42 ml, 1:2:2, v/v/v) under nitrogen. The mixture was stirred (magnetic stirring bar) at reflux (2 cycles, 24 h). After each cycle, the solution was transferred via a cannula (leaving the beads in the solid-phase reaction vessel for another cycle) to a flask, and the resin was washed twice with anhydrous methanol. Evaporation of the solvents *in vacuo* afforded a residue.

For **H-Gly-Val-Ala-Val-[Triazine]-Val-Lys(Boc)-Val-Phe-OMe**, the residue was a white solid which was washed with MeOH (230 mg, overall yield 36%) without any other purification. <sup>1</sup>H NMR (400 MHz, DMSO-*d*<sub>6</sub>, 25°C): δ = 8.42–8.25 (m, 3H, NH), 7.97–7.82 (m, 4H, NH), 7.67–7.55 (m, 2H, NH), 7.25–7.17 (m, 10 H, H aromatic), 6.70–6.67 (m, 3H, NH), 4.48–4.02 (m, 10 H, 7 CH<sub>α</sub>, 2 CH<sub>2</sub>-Ph), 3.53 (s, 5H, MeO, CH<sub>2</sub>), 3.18–2.80 (m, 8H, 4 CH<sub>2</sub>-NH), 2.18–2.06 (m, 2H, CH<sub>2</sub>), 1.96–1.80 (m, 4H, 2 CH<sub>2</sub>), 1.69–1.42 (m, 6H, 4 CH<sub>β</sub>, CH<sub>2</sub>), 1.33 (s, 9H, Boc), 1.27–1.15 (m, 7H, CH<sub>3</sub> Ala, 2 CH<sub>2</sub>), 0.85–0.75 (m, 24H, 8 CH<sub>3</sub> Val); MS (ESI, ion polarity positive): *m/z*: 1273.2 [M<sup>+</sup> + H].

For **H-Val-Lys(Boc)-Val-Phe-[Triazine]-Gly-Val-Ala-Val-OMe**, the residue was purified by flash chromatography on silica gel (cyclohexane/MeOH, 95:5, 90:10, 85:15 then MeOH) and obtained as a white solid (138 mg, overall yield 22%). *R*<sub>f</sub> = 0.30 (CH<sub>2</sub>Cl<sub>2</sub>/MeOH 85:15); <sup>1</sup>H NMR (400 MHz, DMSO-*d*<sub>6</sub>, 25°C): δ = 8.26–7.87 (m, 7H, NH), 7.36–7.27 (m,

10 H, H aromatic), 6.81–6.80 (m, 1H, NH), 4.60–4.45 (m, 5H, 3 CH<sub>α</sub>, CH<sub>2</sub>-Ph), 4.29–4.17 (m, 6H, 4 CH<sub>α</sub>, CH<sub>2</sub>-Ph), 3.82 (m, 2H, CH<sub>2</sub>), 3.72 (s, 3H, MeO), 3.13–2.85 (m, 8H, 4 CH<sub>2</sub>-NH), 2.22–2.00 (m, 7H, 3 CH<sub>β</sub>, 2 CH<sub>2</sub>), 1.98–1.58 (m, 4H, 2 CH<sub>2</sub>), 1.46 (s, 9H, Boc), 1.33–1.29 (m, 8H, CH<sub>3</sub> Ala, CH<sub>β</sub> Ala, 2 CH<sub>2</sub>), 0.97–0.84 (m, 24H, 8 CH<sub>3</sub> Val); MS (ESI, ion polarity positive): *m/z*: 1273.7 [M<sup>+</sup> + H].

### H-Gly-Val-Ala-Val-(Triazine)-Val-Lys-Val-Phe-OMe 1

A solution of compound H-Gly-Val-Ala-Val-[Triazine]-Val-Lys(Boc)-Val-Phe-OMe (230 mg, 0.18 mmol) in MeOH (17 ml) and HCl/MeOH (3.5 ml, 4.9 N) was stirred overnight at room temperature and then concentrated by rotary evaporation to afford the free compound **1** (271 mg, quantitative) as a white solid. This product was purified by preparative HPLC using a linear gradient from solvent A/B (40/60) to A/B (30/70) over 30 min; flow = 6 ml/min; *t<sub>R</sub>* = 14 min 20 s. Product **1** was obtained as a white solid (121 mg, 0.06 mmol, overall yield 12%). C<sub>58</sub>H<sub>92</sub>N<sub>16</sub>O<sub>10</sub>.8 CF<sub>3</sub>COOH (2085.61): calcd C, 42.61; H, 4.83; N, 10.75; found: C, 43.24; H, 5.34; N, 11.46; IR (neat):  $\nu$  = 3279 (NH), 1631 (C=O) 1029 (C-O) cm<sup>-1</sup>; MS (ESI, ion polarity positive): *m/z*: 1173.9 [M<sup>+</sup>], 1175.0 [M<sup>+</sup> + H], 1196.0 [M<sup>+</sup> + H + Na]; HRMS (EI): calcd for C<sub>58</sub>H<sub>93</sub>N<sub>16</sub>O<sub>10</sub> (1173.7261), found (1173.7266); CD : [Compound **1**]<sub>water</sub> = 187 μM, two minima at 200 and 229 nm; [Compound **1**]<sub>HFIP</sub> = 188 μM, two minima at 196 and 229 nm; <sup>1</sup>H NMR (500 MHz, CD<sub>3</sub>OH) and <sup>13</sup>C NMR (125 MHz, CD<sub>3</sub>OH) Table 1.

### H-Val-Lys-Val-Phe-(Triazine)-Gly-Val-Ala-Val-OMe 2

A solution of compound H-Val-Lys(Boc)-Val-Phe-[Triazine]-Gly-Val-Ala-Val-OMe (69 mg, 0.05 mmol) in MeOH (5 ml) and HCl/MeOH (1 ml, 4.17 N) was stirred overnight at room temperature and then concentrated by rotary evaporation to afford the free compound **2** (80 mg, quantitative) as a white solid. This product was purified by preparative HPLC employing a linear gradient from solvent A/B (40/60) to A/B (30/70) over 30 min; flow = 6 ml/min; *t<sub>R</sub>* = 11 min 39 s. Product **2** was obtained as a white solid (19 mg, 0.01 mmol, overall yield 2%). MS (ESI, ion polarity positive): *m/z*: 1173.6 [M<sup>+</sup> + H], 587.4 [M<sup>+</sup> + 2H]/2; CD : [Compound **2**]<sub>water</sub> = 282 μM, a minimum at 196 nm and a maximum at 217 nm; [Compound **2**]<sub>HFIP</sub> = 142 μM, two minima at 196 and 229 nm; <sup>1</sup>H NMR (500 MHz, CD<sub>3</sub>OH) and <sup>13</sup>C NMR (125 MHz, CD<sub>3</sub>OH) (Table 2).

### Supplementary Material

Supplementary electronic material for this paper is available in Wiley InterScience at: <http://www.interscience.wiley.com/jpages/1075-2617/suppmat/>

### Acknowledgements

The MNSER is gratefully thanked for a doctoral fellowship for BD.

### REFERENCES

- Sunde M, Blake CCF. The structure of amyloid fibrils by electron microscopy and X-ray diffraction. *Adv. Protein Chem.* 1997; **50**: 123–159.
- Dobson CM. Structural biology: prying into prion. *Nature* 2005; **435**: 747–749.
- Krishnan R, Lindquist SL. Structural insights into a yeast prion illuminate nucleation and strain diversity. *Nature* 2005; **435**: 765–772.
- Nelson R, Sawaya MR, Balbirnie M, Madsen A, Riekel C, Grothe R, Eisenberg D. Structure of the cross-β spine of amyloid-like fibrils. *Nature* 2005; **435**: 773–778.
- Ritter C, Maddelein ML, Siemer AB, Lührs T, Ernst M, Meier BH, Sauppe SJ, Riek R. Correlation of structural elements and infectivity of the HET-s prion. *Nature* 2005; **435**: 844–848.
- Murphy RM. Peptide aggregation in neurodegenerative disease. *Annu. Rev. Biomed. Eng.* 2002; **4**: 155–174.
- Mager PP, Penke B, Walter R, Harkany T, Härtig W. Pathological peptide folding in Alzheimer's disease and other conformational disorders. *Curr. Med. Chem.* 2002; **9**: 1763–1780. And references therein.
- Harrison PM, Bamborough P, Daggett V, Prusiner SB, Cohen FE. The prion folding problem. *Curr. Opin. Struct. Biol.* 1997; **7**: 53–59.
- Baldwin MA, Cohen FE, Prusiner SB. Prion protein isoforms, a convergence of biological and structural investigations. *J. Biol. Chem.* 1995; **270**: 19197–19200.
- Prusiner SB. Prions. *Proc. Natl. Acad. Sci. U.S.A.* 1998; **95**: 13363–13383.
- Lotharius J, Brundin P. Pathogenesis of Parkinson's disease: dopamine, vesicles and α-synuclein. *Nat. Rev.* 2002; **3**: 1–11. And references therein.
- Westermarck P. Quantitative studies on amyloid in islets of Langerhans. *Ups. J. Med. Sci.* 1972; **77**: 91–94.
- Höppener JWM, Ahrén B, Lips CJM. Islet amyloid and type 2 diabetes mellitus. *N. Engl. J. Med.* 2000; **343**: 411–419.
- Vidal J, Verchere CB, Andrikopoulos S, Wang F, Hull RL, Cnop M, Olin KL, Leboeuf RC, O'Brien KD, Chait A, Kahn SE. The effect of apolipoprotein E deficiency on islet amyloid deposition in human islet amyloid polypeptide transgenic mice. *Diabetologia* 2003; **46**: 71–79.
- Degrado WF, Lear JD. Induction of peptide conformation at apolar water interfaces. A study with model peptides of hydrophobic periodicity. *J. Am. Chem. Soc.* 1985; **107**: 7684–7689.
- Rajasekharan Pillai VI, Mutter M. Conformational studies of poly(oxyethylene)-bound peptides and protein sequences. *Acc. Chem. Res.* 1981; **14**: 122–130.
- Osterman D, Mora R, Kezdy FJ, Kaiser ET, Meredith SC. A synthetic amphiphilic beta-strand tridecapeptide: a model for apolipoprotein B. *J. Am. Chem. Soc.* 1984; **106**: 6845–6847.
- Kemp DS, Bowen BR. Synthesis of peptide-functionalized diacylaminoepindolidiones as template for β-sheet formation. *Tetrahedron Lett.* 1988; **29**: 5077–5080.
- Kemp DS, Bowen BR. Conformational analysis of peptide-functionalized diacylaminoepindolidiones <sup>1</sup>H NMR evidence for β-sheet formation. *Tetrahedron Lett.* 1988; **29**: 5081–5082.
- Kemp DS, Bowen BR, Muendel CC. Synthesis and conformational analysis of epindolidione-derived peptide models for beta-sheet formation. *J. Org. Chem.* 1990; **55**: 4650–4657.
- Martin SF, Austin RE, Oalman CJ, Baker W, Condon SL, deLara E, Rosenberg SH, Spina KP, Stein HH, Cohen J, Kleinfert HD. 1,2,3-trisubstituted cyclopropanes as conformationally restricted peptide isosteres: application to the design and synthesis of novel renin inhibitors. *J. Med. Chem.* 1992; **35**: 1710–1721.
- Smith AB III, Guzman MC, Sprengeler PA, Keenan TP, Holcomb RC, Wood JL, Carroll PJ, Hirschmann R. De novo design, synthesis, and X-ray crystal structures of pyrrolinone-based beta-strand peptidomimetics. *J. Am. Chem. Soc.* 1994; **116**: 9947–9962.

23. Smith AB III, Hirschmann R, Pasternak A, Akaishi R, Guzman MC, Jones DR, Keenan TP, Sprengeler PA. Design and synthesis of peptidomimetic inhibitors of HIV-1 protease and renin. Evidence for improved transport. *J. Med. Chem.* 1994; **37**: 215–218.
24. Smith AB III, Hirschmann R, Pasternak A, Guzman MC, Yokoyama A, Sprengeler PA, Darke PL, Emini EA, Schleif WA. Pyrrolinone-based HIV protease inhibitors. Design, synthesis and antiviral activity: evidence for improved transport. *J. Am. Chem. Soc.* 1995; **117**: 11113–11123.
25. Kirsten CN, Schrader TH. Intermolecular  $\beta$ -sheet stabilization with aminopyrazoles. *J. Am. Chem. Soc.* 1997; **119**: 12061–12068.
26. Rzepecki P, Wehner M, Molt O, Zadnarm R, Harms K, Schrader T. Aminopyrazole oligomers for  $\beta$ -sheet stabilization of peptides. *Synthesis* 2003; 1815–1826.
27. Rzepecki P, Gallmeier H, Geib N, Cernovska K, König B, Schrader T. New heterocyclic  $\beta$ -sheet ligands with peptidic recognition elements. *J. Org. Chem.* 2004; **69**: 5168–5178.
28. Rzepecki P, Nagel-Steger L, Feurstein S, Linne U, Molt O, Zadnarm R, Aschermann K, Wehner M, Schrader T, Riesner D. Prevention of Alzheimer's disease-associated A $\beta$  aggregation by rationally designed nonpeptidic  $\beta$ -sheet ligands. *J. Biol. Chem.* 2004; **279**: 47497–47505.
29. Diaz H, Tsang KY, Choo D, Kelly JW. The design of water soluble  $\beta$ -sheet structure based on a nucleation strategy. *Tetrahedron* 1993; **49**: 3533–3545.
30. Tsang KY, Diaz H, Graciani N, Kelly JW. Hydrophobic cluster formation is necessary for dibenzofuran-based amino acids to function as beta-sheet nucleators. *J. Am. Chem. Soc.* 1994; **116**: 3988–4005.
31. Nesloney CL, Kelly JW. Synthesis and hydrogen bonding capabilities of biphenyl-based amino acids designed to nucleate  $\beta$ -sheet structure. *J. Org. Chem.* 1996; **61**: 3127–3137.
32. Nesloney CL, Kelly JW. A 2,3'-substituted biphenyl-based amino acid facilitates the formation of a monomeric  $\beta$ -hairpin-like structure in aqueous solution at elevated temperature. *J. Am. Chem. Soc.* 1996; **118**: 5836–5845.
33. Nowick JS, Powell NA, Martinez EJ, Smith EM, Noronha G. Molecular scaffolds. Intramolecular hydrogen bonding in a family of di- and triureas. *J. Org. Chem.* 1992; **57**: 3763–3765.
34. Nowick JS, Mahrus S, Smith ER, Ziller JW. Thiourea derivatives of diethylenetriamine as potential templates for the formation of artificial  $\beta$ -sheets. *J. Am. Chem. Soc.* 1996; **118**: 1066–1072.
35. Nowick JS, Holmes DL, Mackin G, Noronha G, Shaka AJ, Smith EM. An artificial  $\beta$ -sheet comprising a molecular scaffold, a  $\beta$ -strand mimic, and a peptide strand. *J. Am. Chem. Soc.* 1996; **118**: 2764–2765.
36. Nowick JS. Chemical models of protein  $\beta$ -sheet. *Acc. Chem. Res.* 1999; **32**: 287–296.
37. Nowick JS, Chung DM, Maitra K, Stigers KD, Sun Y. An unnatural amino acid that mimics a tripeptide  $\beta$ -strand and forms  $\beta$ -sheet like hydrogen-bonded dimers. *J. Am. Chem. Soc.* 2000; **122**: 7654–7661.
38. Nowick JS, Smith EM, Ziller JW, Shaka AJ. Three stranded mixed artificial  $\beta$ -sheets. *Tetrahedron* 2002; **58**: 727–739.
39. Hibbs DE, Hursthouse MB, Jones IG, Jones W, Malik KMA, North M. Synthesis of peptides and pseudopeptides incorporating an endo-(2S,3R)-norborn-5-ene residue as a turn inducer. *J. Org. Chem.* 1998; **63**: 1496–1504.
40. Ranganathan D, Haridas V, Kurur S, Thomas A, Madhusudan KP, Nagaraj R, Kunwar AC, Sarma AV, Karle IL. Demonstration of endo-cis-(2S, 3R)-bicyclo[2.2.1]hept-5-en-2,3- dicarbonyl unit as a reverse-turn scaffold and nucleator of two stranded parallel  $\beta$ -sheet: design, synthesis, crystal structure, and self-assembling properties of norborneno peptide. analogues. *J. Am. Chem. Soc.* 1998; **120**: 8448–8460.
41. Hackenberger CPR, Schiffrers I, Runsink J, Bolm C. General synthesis of unsymmetrical norbornane scaffolds as inducers for hydrogen bond interactions in peptides. *J. Org. Chem.* 2004; **69**: 739–743.
42. Minor DL Jr, Kim PS. Measurement of the  $\beta$ -sheet-forming propensities of amino acids. *Nature* 1994; **367**: 660–663.
43. Löwik DWPM, Lowe CR. A stepwise synthesis of triazine-based macrocyclic scaffolds. *Tetrahedron Lett.* 2000; **41**: 1837–1840.
44. Löwik DWPM, Lowe CR. Synthesis of macrocyclic, triazine-based receptor molecules. *Eur. J. Org. Chem.* 2001; 2825–2839.
45. Yang X, Lowe CR. Synthesis of novel rigid triazine-based calix [6] arenes. *Tetrahedron Lett.* 2003; **44**: 1359–1362.
46. Scharn D, Germeroth L, Schneider-Mergener J, Wenschuh H. Sequential nucleophilic substitution on halogenated triazines, pyrimidines, and purines: a novel approach to cyclic peptidomimetics. *J. Org. Chem.* 2001; **66**: 507–513.
47. Zerkowski JA, Hensley LM, Abramowitz D. Triazinyl-amino-acids, new building blocks for pseudopeptides. *Synlett* 2002; 557–560.
48. Arduini M, Crego-Calama M, Timmerman P, Reinhoudt DN. A novel type of hydrogen-bonded assemblies based on the melamine cyanuric acid motif. *J. Org. Chem.* 2003; **68**: 1097–1106.
49. Simanek EE, Mammen M, Gordon DM, Chin D, Mathias JP, Seto CT, Whitesides GM. Design and synthesis of hydrogen-bonded aggregates. Theory and computation applied to three systems based on the cyanuric acid-melamine lattice. *Tetrahedron* 1995; **51**: 607–619.
50. Zhang W, Nowlan DT III, Thomson LM, Lackowski WM, Simanek EE. Orthogonal convergent synthesis of dendrimers based on melamine with one or two unique surface sites for manipulation. *J. Am. Chem. Soc.* 2001; **123**: 8914–8922.
51. Steffensen MB, Simanek EE. Chemoselective building blocks for dendrimers from relative reactivity data. *Org. Lett.* 2003; **5**: 2359–2361.
52. Henke BR, Consler TG, Go N, Hale RL, Hohman DR, Jones SA, Lu AT, Moore LB, Moore JT, Orband-Miller LA, Robinett RG, Shearin J, Spearing PK, Stewart EL, Turnbull PS, Weaver SL, Williams SP, Wisely GB, Lambert MH. A new series of estrogen receptor modulators that display selectivity for estrogen receptor  $\beta$ . *J. Med. Chem.* 2002; **45**: 5492–5505.
53. Pattarawarapan M, Reyes S, Xia Z, Zaccaro MC, Saragovi HU, Burgess K. Selective formation of Homo- and heterobivalent peptidomimetics. *J. Med. Chem.* 2003; **46**: 3565–3567.
54. Bork JT, Lee JW, Khersonsky SM, Moon HS, Chang YT. Novel orthogonal strategy toward solid-phase synthesis of 1,2,3-substituted triazines. *Org. Lett.* 2003; **5**: 117–120.
55. Hajdük PJ, Dinges J, Schkeryantz JM, Janowick D, Kaminski M, Tufano M, Augeri DJ, Petros A, Nienaber V, Zhong P, Hammond R, Coen M, Beutel B, Katz L, Fesik SW. Novel inhibitors of Erm methyltransferases from NMR and parallel synthesis. *J. Med. Chem.* 1999; **42**: 3852–3859.
56. Baidur N, Chadha N, Brandt BM, Asgari D, Patch RJ, Schalk-HiHi C, Carver TE, Petrounia IP, Baumann CA, Ott H, Manthey C, Springer BA, Player MR. 2-Hydroxy-4,6-diamino- [1,3,5] triazines: a novel class of VEGF-R2 (KDR) tyrosine kinase inhibitors. *J. Med. Chem.* 2005; **48**: 1717–1720.
57. Wang SS. *p*-Alkoxybenzyl alcohol resin and *p*-alkoxybenzyl oxycarbonylhydrazide resin for solid phase synthesis of protected peptide fragments. *J. Am. Chem. Soc.* 1973; **95**: 1328–1333.
58. Hancock WS, Battersby JE. A new micro-test for the detection of incomplete coupling reactions in solid-phase peptide synthesis using 2,4,6-trinitrobenzene-sulphonic acid. *Anal. Biochem.* 1976; **71**: 260–264.
59. Kaiser E, Colescott RL, Bossinger CD, Cook PI. Color test for detection of free terminal amino groups in the solid-phase synthesis of peptides. *Anal. Biochem.* 1970; **34**: 595–598.
60. Carpino LA. 1-Hydroxy-7-azabenzotriazole. An efficient peptide coupling additive. *J. Am. Chem. Soc.* 1993; **115**: 4397–4398.
61. Carpino LA, El-Faham A. Effect of tertiary bases on O-benzotriazolyluronium salt-induced peptide segment coupling. *J. Org. Chem.* 1994; **59**: 695–698.
62. Carpino LA, El-Faham A, Albericio F. Racemization studies during solid-phase peptide synthesis using azabenzotriazole-based coupling reagents. *Tetrahedron Lett.* 1994; **35**: 2279–2282.

63. Carpino LA, El-Faham A. Efficiency in peptide coupling: 1-hydroxy-7-azabenzotriazole vs 3,4-dihydro-3-hydroxy-4-oxo-1,2,3-benzotriazine. *J. Org. Chem.* 1995; **60**: 3561–3564.
64. Gennari C, Mielgo A, Potenza D, Scolastico C, Piarulli U, Manzoni L. Solid-phase synthesis of peptides containing reverse-turn mimetic bicyclic lactams. *Eur. J. Org. Chem.* 1999; 379–388.
65. Chitnumsub P, Fiori WR, Lashuel HA, Diaz H, Kelly JW. The nucleation of monomeric parallel  $\beta$ -sheet-like structures and their self-assembly in aqueous solution. *Bioorg. Med. Chem.* 1999; **7**: 39–59. And references therein.
66. Birkett HE, Robin KH, Hodgkinson P, Carr K, Charlton MH, Cherryman JC, Chippendale AM, Glover RP. NMR studies of exchange between triazine rotamers. *Magn. Reson. Chem.* 2000; **38**: 504–511.
67. Birkett HE, Cherryman JC, Chippendale AM, Hazendonk P, Robin KH. Molecular modelling studies of side-chain rotation in substituted triazine rings. *J. Mol. Struct.* 2002; **602–603**: 59–70.
68. Birkett HE, Cherryman JC, Chippendale AM, Evans JSO, Robin KH, James M, King IJ, McPherson J. Structural investigations of three triazines: solution-state NMR studies of internal rotation and structural information from solid-state NMR, plus a full structure determination from powder x-ray diffraction in one case. *Magn. Reson. Chem.* 2003; **41**: 324–336.
69. Amm M, Platzer N, Guilhem J, Bouchet JP, Volland JP. Structural and conformational study of substituted triazines by  $^{15}\text{N}$  NMR and x-ray analysis. *Magn. Reson. Chem.* 1998; **36**: 587–596.
70. Katritzky J, Oniciu D, Ghiviriga I, Barcock A. 4,6-Bis- and 2,4,6-tris-(*N,N*-dialkylamino)-*s*-triazines: synthesis, NMR spectra and restricted rotations. *J. Chem. Soc., Perkin Trans. 2* 1995; 785–792.
71. Wishart DS, Sykes BD, Richards FM. The chemical shift index: a fast and simple method for the assignment of protein secondary structure through NMR spectroscopy. *Biochemistry* 1992; **31**: 1647–1651.
72. Schwarzinger S, Kroon GJA, Foss TR, Chung J, Wright PE, Dyson HJ. Sequence-dependant correction of random-coil NMR chemical shifts. *J. Am. Chem. Soc.* 2001; **123**: 2970–2978.
73. Smith LJ, Bolin KA, Schwalbe H, MacArthur MW, Thornton JM, Dobson CM. Analysis of main chain torsion angles in proteins: prediction of NMR coupling constants for native and random coil conformations. *J. Mol. Biol.* 1996; **255**: 494–506.
74. Kinoshita M, Okamoto Y, Hirata F. Peptide conformations in alcohol and water: analyses by the reference interaction site model theory. *J. Am. Chem. Soc.* 2000; **122**: 2773–2779.
75. Demonchaux P, Ganellin CR, Dunn PM, Haylett DG, Jenkinson DH. Search for the pharmacophore of the  $\text{K}^+$  channel blocker, apamin. *Eur. J. Med. Chem.* 1991; **26**: 915–920.
76. Bax A, Davis DG. MLEV-17 based two-dimensional homonuclear magnetization transfer spectroscopy. *J. Magn. Reson.* 1995; **65**: 355–360.
77. Hwang TL, Shaka AJ. Cross relaxation without TOCSY: transverse rotating-frame Overhauser effect spectroscopy. *J. Am. Chem. Soc.* 1992; **114**: 3157–3159.
78. Marion D, Wüthrich K. Application of phase sensitive two-dimensional correlated spectroscopy (COSY) for measurements of  $^1\text{H}$ - $^1\text{H}$  spin-spin coupling constants in proteins. *Biochem. Biophys. Res. Commun.* 1983; **113**: 967–974.
79. Schleucher J, Schwendinger M, Griesinger C. A general enhancement scheme in heteronuclear multidimensional NMR employing pulsed field gradients. *J. Biomol. NMR* 1994; **4**: 301–306.
80. Wüthrich K. *NMR of Proteins and Nucleic Acids*. Wiley: New York, 1986.
81. Berlose JP, Convert O, Brunissen A, Chassaing G, Lavielle S. Three-dimensional structure of the highly conserved seventh transmembrane domain of G-protein-coupled receptors. *Eur. J. Biochem.* 1994; **225**: 827–843.
82. Wishart DS, Bigam CG, Holm A, Hodges RS, Sykes BD.  $^1\text{H}$ ,  $^{13}\text{C}$  and  $^{15}\text{N}$  random coil NMR chemical shifts of the common amino acids. Investigations of nearest-neighbor effects. *J. Biomol. NMR* 1995; **5**: 67–81.
83. Braz GI, Antonov VK, Kurdyumova KN. Some ethylenimino-1,3,5-triazines. *Zh. Obshch. Khim.* 1958; **28**: 2972–2975.